

The Smallest Electron Storage Ring for High-Intensity Far-Infrared and Hard X-ray Productions†

H. Yamada

Department of Optronics, College of Science and Engineering, Ritsumeikan University, Nojihigashi, Kusatsu, Shiga 525, Japan. E-mail: hironari@bkc.ritsumei.ac.jp

(Received 4 August 1997; accepted 3 June 1998)

The status of the world's smallest electron storage ring is reported. This ring is designed to provide coherent far-infrared (FIR) and incoherent hard X-ray emissions from a single 50 MeV storage ring. The FIR emission is forced by a surrounding mirror around the electron orbit. The FIR emission mechanism is rather similar to that of the free-electron laser. The expected FIR output is of the order of 100 W. Bremsstrahlung is used instead of synchrotron radiation to generate hard X-rays. Since electrons recirculate and gain energy from the accelerating cavity, the expected hard X-ray brightness exceeds that of a rotating-anode source by about 1000 times or more.

Keywords: smallest electron storage ring; photon storage rings; FIR beams; hard X-ray beams; FIR applications.

1. Introduction

Since the brightest X-ray source, SPring-8, was successfully commissioned, the synchrotron light community has entered a new stage. SPring-8 could be the last of the large-scale synchrotron radiation rings and thus it is timely to discuss some potential targets for accelerator physicists. We need to discuss beyond the third-generation sources. It is also timely to summarize the demands of users. Note that X-ray beams will become more useful when they can provide a new tool for industrial processes. In order to realise this, a table-top ring is required. One of our next targets should be to develop a small X-ray source, which must be a table-top source but must also be as bright as SPring-8.

Storage rings are not only useful in the X-ray region; according to our recent analysis, the far-infrared (FIR) is also a rather attractive wavelength region (Yamada, 1997). In this paper the author invites the reader to consider a new aspect of the electron storage ring: an ultrahigh-intensity FIR light source, which should generate a new research ramification.

It is useful to see how the storage ring compares with other light sources such as rotating-anode X-ray sources and a free-electron lasers (FELs). High-energy X-rays are generated more efficiently by the small rotating-anode source than the synchrotron radiation source although they are not as bright. It is shown in Fig. 1 that the FEL is able to generate an IR peak power of 1 MW but the average output is of the order of 10 mW. High-pressure mercury

lamps are still very useful because of their size and quietness. The most useful feature of the synchrotron light source is its high-duty cycle compared with the FEL, and its small beam size and narrow angular spread compared with the rotating-anode source. Furthermore, the small ring has the advantage of accumulating a large beam current with a smaller number of electrons due to its smaller circumference, and is suitable for forming short bunches (Yamada, 1996a).

The smallest storage ring was proposed by Yamada in 1993 (Yamada, 1993) and has many advantages over the synchrotron light source, the rotating-anode X-ray source and the FEL. These advantages include the high-duty cycle and small beam size. Coherent FIR light is generated by placing a circular mirror concentrically around the exact circular orbit; this is known as the photon storage ring (PhSR) (Yamada, 1989, 1991). This novel instrument is a multiple-function light source based on an exact circular electron storage ring (Yamada, 1990) with an electron energy lower than 50 MeV. An additional function for hard X-ray generation was proposed in 1995 (Yamada, 1996b). The mechanism for generating hard X-rays with such a low-energy ring is bremsstrahlung from a thin (~ 10 μm) wire target placed in the beam orbit. In the following we will call this instrument the smallest ring.

In this paper the importance and usefulness of the ultrahigh-intensity FIR rays are discussed, which will hopefully open up new research fields in biology and chemistry. The principle for hard X-ray generation and preliminary experimental results have already been demonstrated (Yamada *et al.*, 1998). There are already many articles on photon storage rings and their lasing mechanisms, but the calculated spontaneous PhSR spec-

† This paper was presented as an Invited Paper at the 6th International Conference on Synchrotron Radiation Instrumentation (SRI'97) in Himeji, Japan, on 4–8 August 1997.

trum will be shown here for the first time. The smallest ring is under construction and the commissioning is planned for October at the Institute for Molecular Science in Okazaki. The ring is scheduled to be moved from Okazaki to Ritsumeikan University in April 1998, thus establishing the ring as a user facility. The 22 MeV injector microtron has been ordered.

2. Research ramification by the ultrahigh-intensity FIR rays

The applications of FIR rays ranging in wavelength from a few micrometres to 100 μm are rather interesting. We believe that the PhSR will provide an exciting opportunity to study the processes involved in the life cycle, in which temperature and water are the two essential ingredients. Although we have been living with FIR rays since life first appeared on earth, we know very little about the interaction of FIR rays with the living body. This is primarily due to the lack of variable-wavelength intense FIR sources. It is, of course, highly desirable to study the whole living organism rather than the individual components interactively through FIR interactions.

The time evolution involved in molecular and biological dynamics corresponds to wavelengths of a few micrometres to 100 μm (Fleming & Wolynes, 1990). For example, the relaxation time of a molecular vibration is ~ 0.1 –10 ps, the cycle of molecular vibration is ~ 10 –100 fs, the revolution time of a molecule is ~ 1 ps–100 ns, the ionizing time by light and proteins internal motion is >1 ps, and the relaxation time of formation by photosynthesis is 3.5 ps; these are in the wavelength domain favourable for the PhSR.

As high-speed ‘non-radiative’ transitions are said to exist in complicated living bodies, the organic functions of cells formed with numerous proteins result from small changes in the specific state of proteins. These are called ‘non-radiative’ but this means that the transition energy is extremely small. Therefore, living phenomena can hopefully be investigated by using IR and FIR rays to observe the influence of transitions among the different states of organic materials. The main point of study is to examine

how the living cell functions or behaves when a small transition in a specific element is caused directly in organic materials without breaking down the living state by short-wavelength rays.

We can analyze and realise the structures of these states by Raman spectroscopy using visible light, but in this case we cannot see the dynamics of the living organic materials in this way. Since Raman spectroscopy excites almost every state, we cannot examine the meaning of each state. By exciting selectively the individual state with the specific wavelength of FIR rays from the PhSR, we are able to understand the meaning and dynamics of each state.

Water is not just an H_2O molecule but it forms a network structure in biological molecules. States of biological molecules always interact with water, and we cannot ignore the influence on biological activity produced by the water structure. Water has many absorption lines in the submillimetre wavelength range but we do not yet know the physical meaning of these absorption lines. We may excite a specific water structure by irradiating at the specific wavelength and measuring the de-excitation. In this way we are only able to research the network structure of water. To make a specified protein state active, a specific wavelength with extremely narrow bandwidth is necessary. With the PhSR, the wavelength can be changed freely so research can be performed as desired. Its high output power also makes it possible to achieve a wavelength resolution of $\Delta\lambda/\lambda \simeq 10^{-7}$.

We are planning to apply our method to the treatment of diseases. We will be able to use the PhSR by tuning it to the distinctive wavelength which is strongly absorbed by arterioscleroses, cancer and lighiasis (Aizawa, 1995). We expect these materials to disintegrate and to dissolve in water without pain and side effects. Since the PhSR has a high average power, such use should be ideal. It may therefore be possible to open up a new medical treatment in which FIR rays of specific wavelength are irradiated from outside of the human body, if this wavelength has a narrow bandwidth and is not absorbed by water or other proteins.

Summarizing, we expect the introduction of a new research field in biology, medicine and chemistry using high-intensity FIR rays. We will be able to research the living phenomena in a normal state and control externally the function of living organic materials. The PhSR will make this possible.

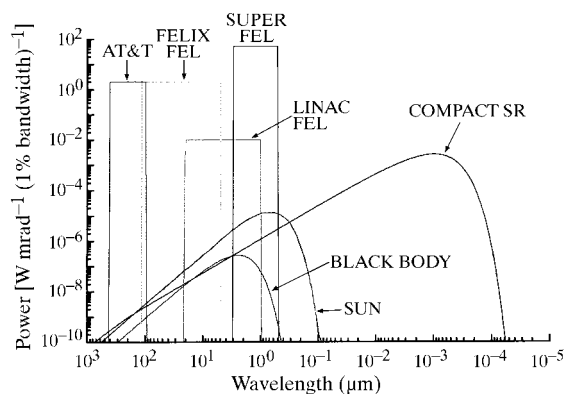


Figure 1
Typical FIR light sources. SR = synchrotron radiation.

3. Construction of the smallest ring

The storage ring under construction has a 0.156 m orbit radius; this is currently the world's smallest storage ring. The magnet has been completed as shown in Fig. 2, which is similar to AURORA (Takahashi, 1987) but is made of normal conducting coils. Two 2.45 GHz accelerator cavities have been completed as shown also in Fig. 3. Due to the limited budget, a 1 kW magnetron is used for the microwave source, whereas a klystron is normally used; we hope

to resolve this limitation in the near future. A 2/3 resonance injection method is introduced, which is similar to the 1/2 integer resonance method (Takayama, 1987) used for AURORA. Two one-turn coils for the kicker magnet have been completed as shown also in Fig. 3. The barrel-shaped mirror made of SiC is in the final stage of fabrication. We are now assembling all these components at the UVSOR booster ring room for the commissioning. The 15 MeV UVSOR linac injector is assigned for this purpose, and the beam-transport system has already been installed.

The accelerator cavity has an unusual shape. A large slit allows synchrotron radiation to pass through. Despite the slit we have obtained the TM01 fundamental mode so to be designed. We could apply almost 0.5 kW power to each cavity. The measured field distribution is shown in Fig. 4. The field was flat to within 5% over a 60 mm-wide span in the transverse direction.

To produce a sufficient kick from a one-turn air-core coil for the 2/3 resonance injection, the maximum 300 G is the necessary field strength for the 15 MeV injection. We have constructed a pulsed power supply which has a 2 μ s half-cycle sine-shaped pulse with a maximum peak current of 4.5 kA. We use a magnetic pulse compression technique using an amorphous core to compress the pulse to 0.4 μ s. We have successfully generated a pulse of less than 0.4 μ s.

4. PhSR output

Since it is too early to demonstrate the experimental PhSR spectrum, we present the calculated spontaneous coherent spectrum. Similar to the spontaneous undulator spectrum, we expect to obtain a good agreement between calculated and experimental spontaneous PhSR spectra. The spectrum is given by

$$\begin{aligned} P(\lambda) d\Omega d\lambda &= p(\lambda) h N_e [1 + (N_e - 1) F(\lambda)] G(\lambda) d\Omega d\lambda \\ &\simeq p(\lambda) h N_e [1 + N_e F(\lambda)] G(\lambda) d\Omega d\lambda, \end{aligned} \quad (1)$$

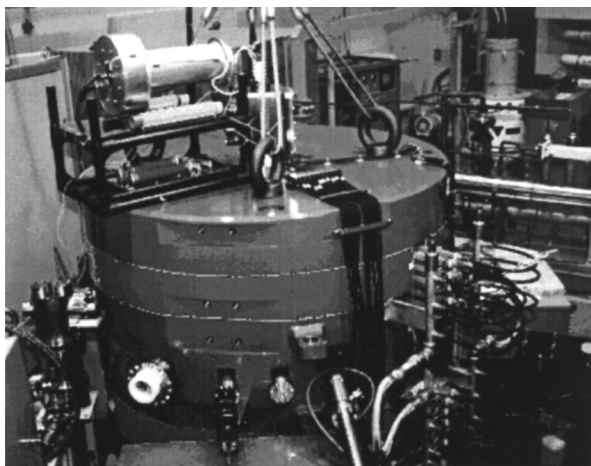


Figure 2

Overview of the storage ring scheduled to become operational at Ritsumeikan University in 1998. This is currently the world's smallest synchrotron radiation source.

where $p(\lambda)$ is the incoherent synchrotron radiation power from one electron, h is the harmonic number and N_e is the number of electrons in the bunch; thus, hN_e gives the beam current and $p(\lambda)hN_e$ gives the normal incoherent synchrotron radiation power in mrad at a certain bandwidth. $F(\lambda)$ is a form factor which is the Fourier transform of the longitudinal electron distribution in the bunch. If a Gaussian electron distribution is assumed, F is given as

$$F(\lambda) = \exp[-(2\pi\sigma_L/\lambda)^2], \quad (2)$$

where σ_L is the r.m.s. bunch length. The function $G(\lambda)$ represents the interference between the coherent rays as well as between the incoherent rays as a result of the reflection due to the surrounding mirror. This is given for a certain reflection coefficient f as

$$\begin{aligned} G(\lambda) &= \left[\sum_r^{N_b} (f^{1/2})^r \sin(r\pi\lambda/\lambda_R) / \sin(\pi\lambda/\lambda_R) \right]^2 \\ &\simeq \left[\sum_r^{N_b} (f^{1/2})^r \right]^2 [\sin(\hat{N}\pi\lambda/\lambda_R) / \sin(\pi\lambda/\lambda_R)]^2 \\ &\simeq [1/(1 - f^{1/2})]^2 \delta(\lambda/\lambda_R) \quad (N_b = \infty). \end{aligned} \quad (3)$$

Here, the phase slippage between rays from different bunches is assumed to be negligible. The coherent synchrotron radiation power from the PhSR is proportional to the square of the electron number, N_e , in the bunch, and to the square of the averaged number of interaction times, \hat{N} . The resonating wavelength, λ_R , is given by

$$(m + 1/2)\lambda_R = 2(\theta + n\pi/h)\rho/\beta_0 - 2\rho \cos \alpha \tan \theta, \quad (4)$$

where ρ is the orbit radius, m is the higher harmonic number and θ is related to the mirror radius, R_m , by

$$R_m = \rho \cos \alpha / \cos \theta. \quad (5)$$

In Fig. 5 the calculated spontaneous PhSR spectrum is shown. The calculation is based on the following conditions: beam current, 1 A; bunch length, 0.5 mm in one

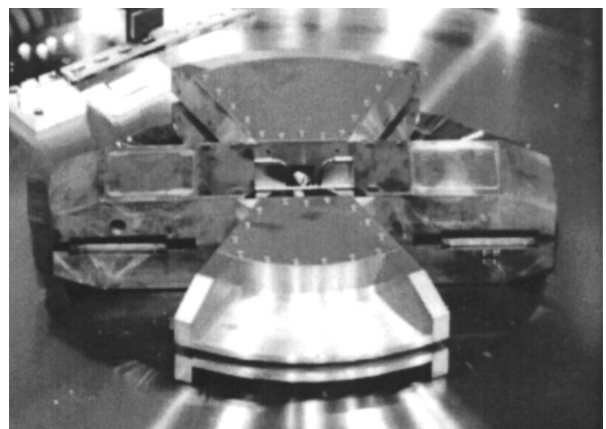


Figure 3

A pair of accelerating cavities (on the left and right) and two perturber coils (at the top and bottom) are installed in the vacuum chamber. The cavity has a wide slit to allow rays to pass through. The perturber is a one-turn coil.

standard deviation; power extraction efficiency, 30%; resonance wavelength, 30 μm ; average number of interactions, 100 for a wavelength of 10 μm . We see peaks at the fundamental and the higher harmonic wavelengths. Since the mirror is assumed to be truly circular, we should be able to see these higher harmonics up to very short wavelengths. However, depending on the tolerance of the mirror radius, it may not be possible to see these higher harmonics.

The accuracy of the mirror radius is more important than the surface roughness. The total phase shift, $\Delta\lambda$, is related to the maximum error of the mirror radius, ΔR_r , according to

$$\Delta\lambda = \left[\sum_n (\Delta\lambda_n)^2 \right]^{1/2} \\ \simeq (2\rho^2/R_0^2)\Delta_r \left\{ \sum_n [\sin(n\theta/2\pi q)/\sin(n\theta)]^2 \right\}^{1/2},$$

where $\Delta\lambda_n$ is the individual shift, q is an integer and n is the number of reflections. The error, ΔR_m , is assumed to have the function

$$\Delta R_m = \Delta_r \sin(\theta/2\pi q).$$

The acceptable error of the mirror radius is $\Delta_r = \pm 0.1 \mu\text{m}$ for lasing at a wavelength of 30 μm , which keeps the phase shift within 10% after reflecting 100 times.

The expected output is approximately 1 W of spontaneous emission and is similar to the brightest sources in the FIR region. When the beam current is low, the bunch length becomes as small as 0.1 mm because the intrabeam scattering effect becomes small. For 1 mA beam current, the coherent synchrotron radiation emission is enhanced at wavelengths longer than 100 μm as shown in Fig. 6. The accumulation of a large beam current in the low-energy ring introduces beam-instability problems and requires substantial effort in optimizing the ring operating conditions. However, with only 10 mA beam current, we can generate an average power of 1 mW, which is equivalent to the average power of the FEL.

The above discussion concerns spontaneous emission but not laser emission. Strictly speaking, we are unable to distinguish between spontaneous and laser emissions since

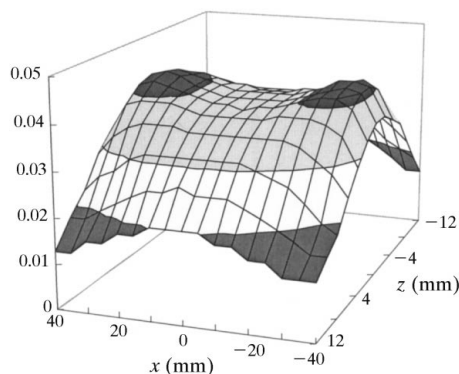


Figure 4 Electric field distribution along the accelerating gap (z direction) in the radial direction (x direction).

the circular mirror functions as a laser cavity simultaneously. Lasing occurs when the phase velocities of the electrons and the electromagnetic waves are the same (Mima *et al.*, 1991).

5. Hard X-ray generation

Photon emission is a quantum mechanical process namely by the electron. Regardless of the magnetic or electric forces, the emission occurs due to the acceleration of an electron. In any case the characteristics of the emission is simply determined by the energy and momentum conservation laws. Bremsstrahlung should be emitted in a strongly forward direction in a $1/\gamma$ cone, the same as with synchrotron radiation, if the electron energy is relativistic. High-energy X-rays can be generated more easily by bremsstrahlung than by synchrotron radiation, since the atomic Coulomb force is much stronger in the vicinity of the nucleus than the magnetic field of a bending magnet. It is believed that the electron must be stopped in the target, similar to in X-ray tubes. If this is true, then there are no advantages for using the storage ring to generate bremsstrahlung. Some researchers have used thick targets with a linac to generate hard X-rays, but in this case forward focusing is lost because of the straggling of electrons. We have found that a thin-target X-ray beam has forward focusing, and the electron recirculates in the storage ring as predicted by Yamada (1996b).

The experiment was carried out on SOR-Ring at ISSP, which was the first Japanese synchrotron light source (Ishii, 1994). Since this facility was closed immediately after this experiment, we could celebrate the ring's final duty with this unusual experiment, which was intended to help to prepare the new-generation light source. The experiment was carried out by inserting quickly a 10 μm -diameter Ni wire or a 10 μm -thick \times 3 mm-wide Be film into the beam orbit and measuring the beam current, the X-ray beam profile and the X-ray energy spectrum through a 1 mm-thick aluminium window. The experiment was undertaken with electron energies of 300, 380 and 500 MeV. The photoelectric current was observed to monitor the beam

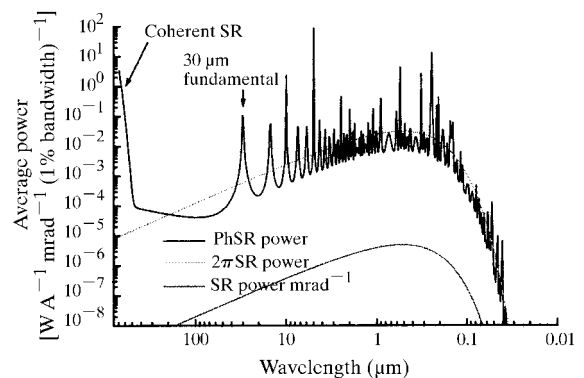


Figure 5 Spontaneous coherent radiation spectrum at 1 A beam current. SR = synchrotron radiation.

Table 1
RF power dependence of the integrated beam current.

RF power (W)	Beam current (mA)	Electron number	Integrated charge hitting target (mC)	Total electron number hitting target
548	9	3.51×10^9	19	1.2×10^{17}
263	10	3.89×10^9	21	1.37×10^{17}
94	10	3.95×10^9	21	1.36×10^{17}
28	10	3.69×10^9	17	1.06×10^{17}

current. A digital oscilloscope was used since the lifetime is too short to use a conventional beam-monitor system. The time variation of the beam current is shown in Fig. 7 for four different accelerating powers. The observed beam lifetime is nearly 2 s. We found that the beam lifetime was extended when the accelerating power was increased and was saturated at 548 W, which implies that electrons are recirculating.

If all electrons are stopped by the target at one time, the generated photon number is simply proportional to the electron number in the bunch, which is of the order of 10^{10} . If we have a 1 s beam lifetime, the beam hits the target 10^8 times, which is the revolution frequency. This corresponds to 10^{17} hits on the target before all electrons are terminated. The electrons are terminated when each energy loss and angular deviation is larger than the momentum acceptance and the dynamic aperture. The experimentally observed values are shown in Table 1 for different accelerating powers, and are quite consistent with our expectation. In this method, high-energy X-rays are generated up to the electron energy; thus the generated X-rays are not all useful, but it is a useful amount.

The beam lifetime is only 1 s but this is long enough because we have a continuous beam injection by using the resonance injection method. The calculated X-ray intensity of this new X-ray source is shown in Fig. 8. In this calculation the following parameters were used: 50 Hz injection rate, 10 A peak current, 0.6% injection efficiency, 10 μm -thick tungsten wire, 6% half-momentum aperture, 3 cm chamber radius. It should be stressed that the smallest ring

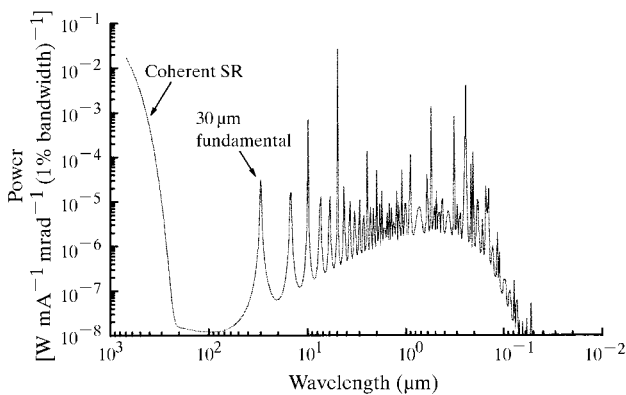


Figure 6
Spontaneous coherent radiation spectrum at 1 mA beam current. SR = synchrotron radiation.

has a very large dynamic aperture and momentum aperture. This is essential for the new source.

Since the number of X-rays was too great and the energy was too high, in this experiment the 10 mm-diameter small NaI detector stopped counting even at a beam current of a few mA. We had to place a 20 cm-thick lead block in front to reduce the count rate, and thus the spectrum measurement was unsuccessful. We therefore plan to use an X-ray monochromator in the next experiment with the 'smallest' storage ring.

6. Summary

Many advances of the table-top storage ring are discussed in this paper, which are summarized in Table 2. It is likely to be one of the brightest sources of FIR rays, aided by the surrounding circular mirror. The intense FIR is expected to open up a new research field. We expect that intense FIR radiation will provide not only a new means for analysis but also for controlling chemical reactions. A new method utilizing bremsstrahlung to generate intense hard X-rays is

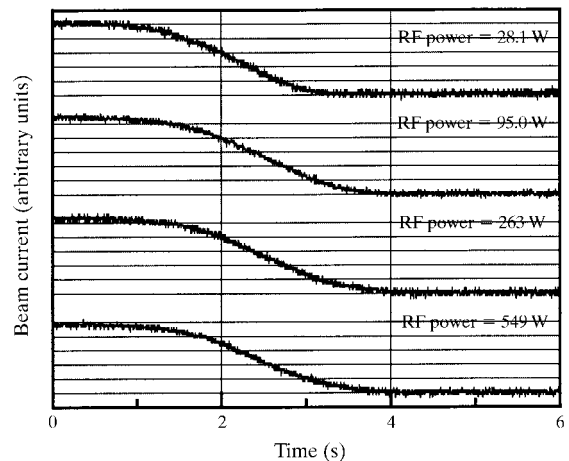


Figure 7
RF power dependence of the beam current.

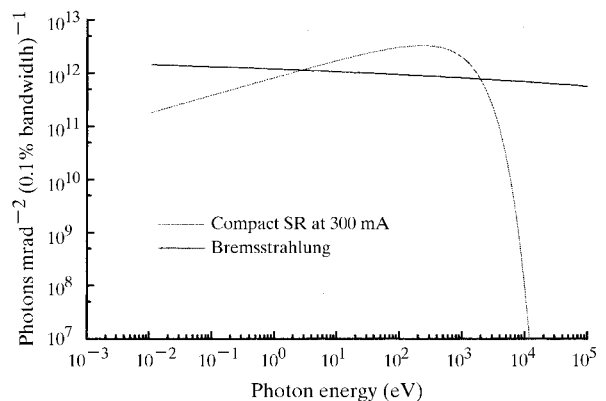


Figure 8
Calculated hard X-ray spectrum from the smallest ring, which is compared with that of the typical superconducting synchrotron radiation (SR) ring.

Table 2

Advanced features of the smallest ring.

High-duty cycle	2.45 GHz
Low-energy electron beam	<50 MeV
Large dynamic aperture	Horizontal: 10 cm; vertical: 6 cm
Large-momentum aperture	6%
Resonance injection method	Enabling continuous injection without disturbing electrons in a central orbit
Short bunch	0.1 mm
Coherent IR and FIR	Similar to free-electron laser
Hard X-ray	1000 times brighter than rotating anode
Instrument size	1 × 3 m (include injector)

verified. The 'smallest' ring has the advantage of being dedicated to private industrial use and can be located as part of an industrial plant.

The author wishes to acknowledge the collaborators who contributed to this project at different stages: Professor Shimoda (formerly of Tokyo University), Professor K. Mima (Osaka University), H. Tsutsui (Sumitomo Heavy Industries Ltd.) and Professors A. I. Kleev and A. B. Manenkov (P. L. Kapitza Institute of Physical Problems) in the photon storage ring theory; T. Takayama, H. Tsutsui, D. Amano and H. Miyade (Sumitomo Heavy Industries Ltd.) in the designing of the smallest storage ring; graduate student I. Sakai and undergraduate students M. Idaka, H. Itoh, H. Shiozaki (Ritsumeikan University), and Dr J. Z. Chen (Hamamatsu Hotonics Inc.) and Y. Tanino (Nihon Pillar Co.) in the construction and testing; Professor H.

Hama, Dr M. Hosaka and J. Yamazaki (UVSOR, Institute for Molecular Science) in the preparation of the injector and commissioning; Drs T. Koseki, H. Takaki and K. Shinoe (Tokyo University) and N. Kawahara, T. Utaka, K. Inaba and T. Omote (Rigaku Inc.) in the hard X-ray generation testing; and Professors Itoh (Kagawa University) and K. Aizawa (Tokyo Medical University) in the search for the FIR applications.

References

- Aizawa, K. (1995). Private communication.
- Fleming, G. R. & Wolyne, P. G. (1990). *Phys. Today*, pp. 36–42.
- Ishii, I. (1994). *Synchrotron Radiation Facilities in Asia*, pp. 45–56. Tokyo: IONICS Publishing.
- Mima, K., Shimoda, K. & Yamada, H. (1991). *IEEE J. Quant. Electron.* **27**, 2572–2577.
- Takahashi, N. (1987). *Nucl. Instrum. Methods Phys. Res. B*, **24/25**, 425–428.
- Takayama, T. (1987). *Nucl. Instrum. Methods*, **24/25**, 420–423.
- Yamada, H. (1989). *Jpn. J. Appl. Phys.* **28**(9), L1665.
- Yamada, H. (1990). *J. Vac. Sci. Technol.* **B8**(6), 1628–1632.
- Yamada, H. (1991). *Nucl. Instrum. Methods Phys. Res. A*, **304**, 700–702.
- Yamada, H. (1993). *Nucl. Instrum. Methods Phys. Res. B*, **79**, 762–766.
- Yamada, H. (1996a). *AIP Conf. Proc.* **367**, 165–180.
- Yamada, H. (1996b). *Jpn. J. Appl. Phys.* **35**, L182–185.
- Yamada, H. (1997). *Adv. Colloid Interface Sci.* **71/72**, 371–392.
- Yamada, H., Sakai, I., Koseki, T., Takaki, H., Shinoe, K., Kawahara, N., Utaka, T., Inaba, K. & Omote, T. (1998). *ISSP Annual Report*. To be published.